

# Regioselective Oxazolation of $C_{70}^{2-}$ and Formation of *cis*-1 $C_{70}$ Adduct with Respect to the Apical Pentagon

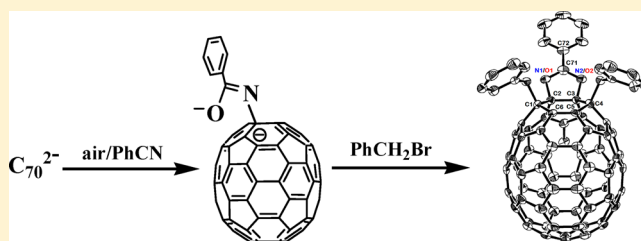
Ling Ni,<sup>†</sup> Wei-Wei Yang,<sup>†</sup> Zong-Jun Li,<sup>†</sup> Di Wu,<sup>‡</sup> and Xiang Gao<sup>\*,†</sup>

<sup>†</sup>State Key Laboratory of Electroanalytical Chemistry, Changchun Institute of Applied Chemistry, Graduate School of Chinese Academy of Sciences, Chinese Academy of Sciences, 5625 Renmin Street, Changchun, Jilin 130022, China

<sup>‡</sup>School of Computer Science and Information Technology, Northeast Normal University, 2555 Jingyue Street, Changchun, Jilin 130117, China

## Supporting Information

**ABSTRACT:** Oxazolation of  $C_{70}$  has been achieved via the aerobic oxidation of  $C_{70}^{2-}$  in the presence of PhCN. Only one  $C_{70}$  oxazoline regioisomer (**1**) is obtained, indicating that the oxazolation of  $C_{70}^{2-}$  occurs with an unusual regioselectivity. Further benzylation of **1**<sup>2-</sup> with benzyl bromide leads to the formation of the first *cis*-1  $C_{70}$  derivative with respect to the apical pentagon (**2**), as shown by the X-ray single-crystal structure and various spectral characterizations. The structure of the obtained  $C_{70}$  oxazoline (**1**) is resolved with H/D labeling benzylation and HMBC (heteronuclear multiple bond coherence) NMR on the basis of the structure of **2**. The result shows that for compound **1**, the O atom is selectively bonded to the C1, while the N atom is bonded to the C2 of  $C_{70}$ . The exhibited regioselectivity for the orientation of oxazolino group on  $C_{70}$  is further rationalized with computational calculations, and a reaction mechanism for the oxazolation of  $C_{70}^{2-}$  is proposed.



## INTRODUCTION

$C_{70}$  and  $C_{60}$  have shown similar reactivities,<sup>1</sup> and they both undergo Bingel,<sup>2,3</sup> Prato,<sup>4,5</sup> Diels–Alder,<sup>6,7</sup> reductive hydrogenation,<sup>8,9</sup> and isoxazolation reactions.<sup>10,11</sup> In addition, both molecules are electron-deficient as demonstrated by similar reductive cyclic voltammetry<sup>12</sup> and can be readily reduced to form stable dianionic species, which can be used for further functionalizations.<sup>13–15</sup> However,  $C_{70}$  differentiates from  $C_{60}$  by having a lower symmetry ( $D_{5h}$  vs  $I_h$ ) and has a much more complex regiochemistry,<sup>16</sup> which has drawn interest in improving the regioselectivity for functionalization.<sup>17,18</sup> Because of the lower symmetry of  $C_{70}$ , regioisomers can be formed for the monocycloaddition of the molecule, not only because the existence of different reactive [6,6]-bonds<sup>16</sup> but also because the possible different orientations when addends with  $C_s$  or lower symmetry are added.<sup>11,16</sup> In addition, the preferred configuration for the bisadduct of  $C_{70}$  differs from that of  $C_{60}$ . The *cis*-1 configuration is one of the most favorable structures for the double additions to  $C_{60}$  as long as the addends are not bulky.<sup>19</sup> However, double additions to  $C_{70}$  usually prefer to have the two addends positioned at the two different poles of  $C_{70}$ , rather than to have them positioned at one pole with a *cis*-1 pattern.<sup>16</sup> To the best of our knowledge, no *cis*-1  $C_{70}$  bisadduct with respect to the apical pentagon of  $C_{70}$  has been reported to date.

Considering the fact that  $C_{70}$  derivatives have shown a better performance than  $C_{60}$  counterparts as organic electronic materials,<sup>20,21</sup> it is of interest to probe further into the regiochemistry of  $C_{70}$  and to prepare  $C_{70}$  derivatives with novel

structures. We have recently reported the preparation of  $C_{60}$  oxazolines via the oxidation of anionic fullerenes in PhCN,<sup>22–24</sup> and a dibenzylated  $C_{60}$  oxazoline with *cis*-1 configuration is obtained upon further benzylation via the charge-directed mechanism.<sup>22,24,25</sup> It is therefore of interest to apply this protocol to the more complex  $C_{70}$  system, to examine the regioselectivity of the reaction, and to examine if it may produce a  $C_{70}$  derivative with *cis*-1 configuration.

## RESULTS AND DISCUSSION

**Regioselective Oxazolation of  $C_{70}^{2-}$  and Characterization of  $C_{70}$  Oxazoline.** Typically,  $C_{70}^{2-}$  was generated by controlled-potential bulk electrolysis (−1.00 V vs SCE) in PhCN containing 0.1 M TBAP (tetra-*n*-butylammonium perchlorate).<sup>14</sup>  $C_{70}$  oxazoline was then obtained via introduction of air into the system, followed by  $I_2$  oxidation of anionic solution, and details are described in the Experimental Section. The crude products were partially soluble in toluene, and the soluble part was purified over a Buckyprep HPLC column, while the insoluble part was likely due to the polymerization involving anionic fullerene epoxide species.<sup>26,27</sup> Two major fractions corresponding to **1** ( $C_{70}$  oxazoline) and unreacted  $C_{70}$  were shown in the HPLC trace (Figure S1, Supporting Information), and compound **1** was obtained with an isolated yield of 16%.

Received: May 17, 2012

Published: August 7, 2012

Positive ESI FT-ICR MS (electrospray ionization Fourier transform ion cyclotron resonance mass spectrometry) of **1** (Figure S2, Supporting Information) shows a monoisotopic peak at  $m/z = 960.04616$ , consistent with the formation of  $C_{70}$  oxazoline ( $C_{77}H_3NO$ ,  $[M + H]^+$  calcd 960.04439). The  $^1H$  NMR (Figure S3, Supporting Information) of the compound shows resonances at 7.94 (d, 2H), 7.35 (t, 1H), and 7.27 (t, 2H) ppm, which correspond to the phenyl protons of the oxazolino heterocycle, while no aliphatic proton resonances are observed in the spectrum, in agreement with the structural assignment.

Figure 1 shows the  $^{13}C$  NMR of the obtained  $C_{70}$  oxazoline (**1**). In the  $sp^3$  carbon region, two weak resonances appear at

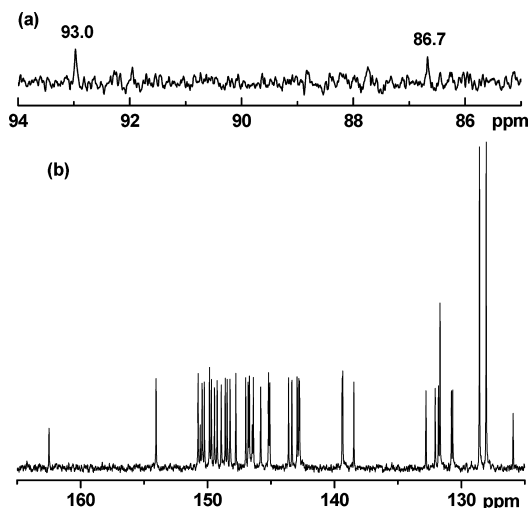


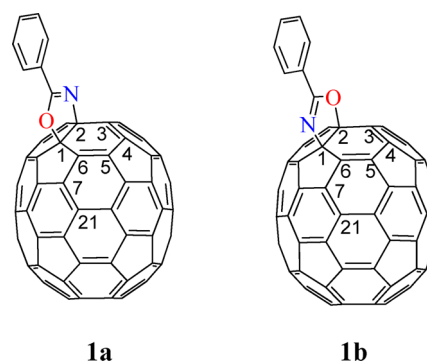
**Figure 1.**  $^{13}C$  NMR of product **1** recorded on a 150 MHz instrument: (a) the  $sp^3$  carbon region; (b) the  $sp^2$  carbon region.

86.7 and 93.0 ppm, which are due to the  $sp^3$   $C_{70}$  carbons bonded to the heteroatoms of nitrogen and oxygen, as observed for the  $C_{60}$  oxazoline compounds.<sup>22–25,28–30</sup> In the  $sp^2$  carbon region, a total of 40 resonances are shown in the spectrum, out of which 35 resonances are due to the  $sp^2$   $C_{70}$  carbons and four resonances are attributed to the phenyl carbons of the oxazolino group, indicating that the compound has a  $C_5$  symmetry with the symmetry plane containing the  $C_5$ -axis of  $C_{70}$ , which provides a key evidence that the oxazolino functionality is bonded to the C1 and C2 of  $C_{70}$ .<sup>31</sup> The most downfield peak resonating at 162.5 ppm originates from the imine carbon of the oxazolino group, consistent with the resonance for  $C_{60}$  oxazolines.<sup>22–25,28–30</sup>

The formation of a C1–C2  $C_{70}$  adduct is further supported by the UV–vis spectroscopic measurement (Figure S5, Supporting Information), which has been shown to be sensitive to the addition pattern rather than the types of addends.<sup>15,32–36</sup> The UV–vis spectrum of the compound shows the typical absorptions for C1–C2 adducts, with absorption bands at 343, 400, 465, 538, and 660 nm.

Notably, there is only one set of resonances for the carbon atoms of  $C_{70}$  in the  $^{13}C$  NMR spectrum and only one major HPLC fraction for the crude product, implying that only one regioisomer is formed from the reaction. Since there are two possible orientations for the oxazolino group on  $C_{70}$  sphere as shown in Scheme 1, it indicates that the oxazolation of  $C_{70}^{2-}$  is highly regioselective for not only excluding the formation of possible C5–C6 and C7–C21 adducts<sup>16</sup> but also for the

**Scheme 1.** Illustrated Structures for the Two Possible C1–C2  $C_{70}$  Oxazoline Regioisomers



formation of only one C1–C2 regioisomer out of two possible structures.

However, it is unlikely to differentiate the two regioisomers only on the basis of the spectral characterizations of the compound itself; even the X-ray single-crystal crystallography of the compound may not be able to discern **1a** and **1b** unambiguously because of the similar electron density of O and N atoms.<sup>23</sup> A similar situation has been reported for the  $C_{70}$  thioethynamine monoadduct.<sup>37</sup> We have recently shown that the heteroatoms of the oxazolino cycle can be discerned with the use of H/D labeling benzylation coupled with HMBC NMR,<sup>25</sup> which allows us to apply this strategy to discern the otherwise unresolved **1a** and **1b**.

#### Formation and Characterization of the *cis*-1 $C_{70}$ Derivative with Respect to the Apical Pentagon.

Compound **2**, a *cis*-1  $C_{70}$  derivative with respect to the apical pentagon, is obtained from the benzylation of dianionic **1**, which can be generated either in situ via the aerobic oxidation of  $C_{70}^{2-}$  in PhCN or via the controlled-potential bulk electrolysis of **1** at  $-1.00$  V vs SCE according to the cyclic voltammogram (CV) of **1** (Figure S6, Supporting Information), even though the reduction is complicated probably by the reductive cleavage of the  $C_{70}$ –O bond, as observed for the  $C_{60}$  counterpart.<sup>25</sup> An isolated yield of 22% was obtained for compound **2** via direct benzylation of oxygenated  $C_{70}^{2-}$ /PhCN solution, while an isolated yield of 37% was obtained from the benzylation of  $1^{2-}$  (see the Experimental Section for details, Figure S7 (Supporting Information) for HPLC).

Figure 2 shows the X-ray single-crystal structure of compound **2**. The results show that a *cis*-1  $C_{70}$  derivative with respect to the apical pentagon is obtained. Because of the similar electron density of the N and O atoms, the nitrogen and oxygen atoms on the  $C_{70}$  sphere cannot be differentiated. In fact, compound **2** should be composed of a 1:1 mixture of two mirror-image enantiomers. Apparently, the oxazolino heterocycle undergoes a rearrangement from C1–C2 to C2–C3 during the transformation from **1** to **2**, consistent with the rearrangement observed for the oxazolino heterocycle on  $C_{60}$  sphere during a similar reaction.<sup>25</sup>

The formation of compound **2** is further supported by accurate MS,  $^1H$  and  $^{13}C$  NMR, and HMBC NMR. The positive ESI FT-ICR MS of compound **2** (Figure S8, Supporting Information) shows the monoisotopic ion peak at  $m/z = 1142.15532$ , in agreement with the formation of  $C_{91}H_{19}NO$  (calcd for  $[M + H]^+$  1142.15394). The  $^1H$  NMR of compound **2** (Figure S9, Supporting Information) shows two AB quartets centered at 3.30 ppm (I,  $AB_q$ ,  $\Delta\nu_{AB} = 421$  Hz,  $J_{AB}$

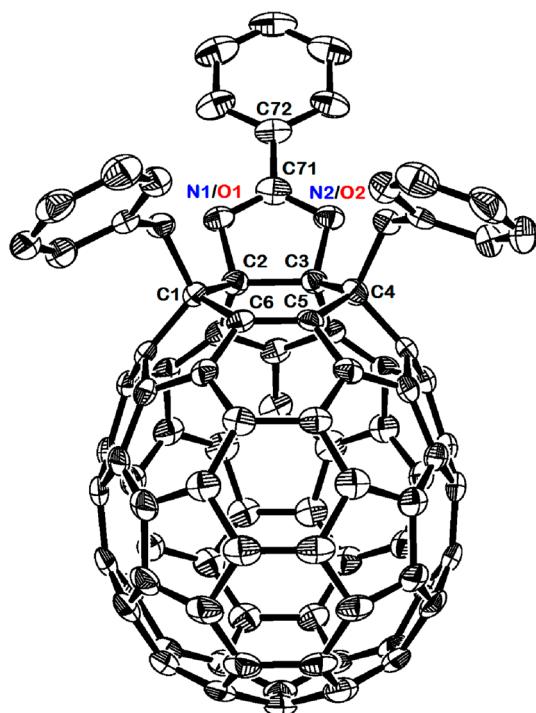


**Figure 2.** ORTEP drawing of compound **2** with 50% thermal ellipsoids. Hydrogen atoms were omitted for clarity. Selected bond distances (Å) and bond angles (deg): C1–C2, 1.592(4); C2–C3, 1.610(5); C3–C4, 1.588(4); C4–C5, 1.519(4); C5–C6, 1.355(4); C6–C1, 1.521(4); C2–N1/O1, 1.470(4); N1/O1–C71, 1.312(4); C71–N2/O2, 1.317(4); N2/O2–C3, 1.454(4); N1/O1–C71–N2/O2, 118.6(3); N1/O1–C71–C72, 120.8(3); N2/O2–C71–C72, 120.6(3).

= 13.2 Hz, 2H) and 3.21 ppm (II, AB<sub>q</sub>,  $\Delta\nu_{AB}$  = 382 Hz,  $J_{AB}$  = 13.2 Hz, 2H), which are due to the diastereotopic methylene protons of the dibenzyls. Resonances arising from the phenyl protons of the oxazolino group are shown at 7.99 (d, 2H), 7.39 (t, 1H), and 7.34 (t, 2H) ppm, while those of the dibenzyls are shown from 6.79 to 6.72 (m, 10H) ppm.

As for the <sup>13</sup>C NMR of **2** (Figure S10, Supporting Information), there are 59 resonances ranging from 164.65 to 131.04 ppm for the sp<sup>2</sup> carbons of C<sub>70</sub> and 12 resonances for the phenyl groups from 130.99 to 126.19 ppm, consistent with the C<sub>1</sub> symmetry of the molecule. The resonance at 161.47 ppm is assigned to the imine carbon of the oxazolino heterocycle as evidenced by the cross peak with the resonance at 7.99 ppm in HMBC NMR (Figure S12, Supporting Information), which corresponds to the <sup>3</sup>J<sub>CH</sub> correlation between the phenyl proton of the oxazoline and the imine carbon. The two most downfield resonances (164.65 and 163.13 ppm) are due to the sp<sup>2</sup> C<sub>70</sub> carbon atoms at the functionalized hexagon of C<sub>70</sub> (C5 and C6 in Figure 2) as derived from the HMBC NMR, where these two resonances show <sup>3</sup>J<sub>CH</sub> correlations with the methylene protons of the benzyl groups respectively, consistent with previous <sup>13</sup>C INADEQUATE NMR result that the most downfield resonances are immediately adjacent to the sp<sup>3</sup> carbons of fullerene.<sup>38</sup>

In the sp<sup>3</sup> carbon region, a total of six resonances are seen in the spectrum. Resonances at 41.92 and 42.99 ppm correspond to the methylene carbons of the two benzyl groups, while those at 57.00 and 57.68 ppm are due to the sp<sup>3</sup> carbons of C<sub>70</sub> bonding to the benzyls. The most notable resonances in the

spectrum are the ones at 84.95 and 92.46 ppm, which are due to the two sp<sup>3</sup> C<sub>70</sub> carbons (C2 and C3) bonded to the heteroatoms of nitrogen and oxygen. It has been shown for the five-membered heterocyclic C<sub>60</sub> and C<sub>70</sub> derivatives, the resonances of the sp<sup>3</sup> fullerene carbon atoms bonded to an oxygen atom range from about 104 to 94 ppm,<sup>10,11,22,23,28,30,39,40</sup> while the resonances of the sp<sup>3</sup> fullerene carbon atoms bonded to a nitrogen atom vary from about 100 to 80 ppm,<sup>22,23,28,41,42</sup> it is therefore rational to assign the resonances at 92.46 and 84.95 ppm to the C<sub>70</sub> sp<sup>3</sup> carbon atoms bonded to the O and N atoms, respectively.

Figure 3 displays the expanded HMBC NMR spectrum of compound **2**. The spectrum shows that the AB quartet I (Ia

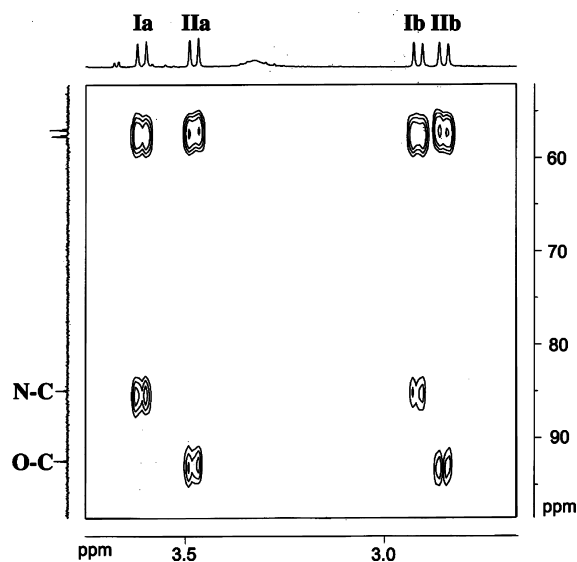


**Figure 3.** Expanded HMBC NMR spectrum of compound **2** recorded in CS<sub>2</sub> with DMSO-*d*<sub>6</sub> as the external lock.

and Ib) are coupled with the sp<sup>3</sup> C<sub>70</sub> carbon bonded to the N atom ( $\delta$  = 84.95 ppm); while the AB quartet II (IIa and IIb) are coupled with the sp<sup>3</sup> C<sub>70</sub> carbon bonded to the O atom ( $\delta$  = 92.46 ppm), indicating that the benzyl corresponding to AB quartet I is positioned next to the N–C<sub>70</sub> bond, while the benzyl corresponding to AB quartet II is located adjacent to the O–C<sub>70</sub> bond. Interestingly, the methylene protons located adjacent to the N–C<sub>70</sub> bond are less shielded with respect to the methylene protons positioned next to the O–C<sub>70</sub> bond, similar to the case observed for the C<sub>60</sub> counterpart,<sup>25</sup> consistent with previous suggestions that the intramolecular CH<sub>2</sub>⋯N interaction is greater than that of CH<sub>2</sub>⋯O in the molecule.<sup>43</sup>

**H/D Labeling Benzilation of 1<sup>2-</sup> and Structure Elucidation of Compound 1.** The H/D labeling benzilation was performed via the reaction of 1<sup>2-</sup> with PhCH<sub>2</sub>Br/PhCD<sub>2</sub>Br in a similar manner as previously reported.<sup>25</sup> The use of both PhCH<sub>2</sub>Br and PhCD<sub>2</sub>Br can help to distinguish the benzyls added to 1<sup>2-</sup> at different steps of the reaction, by taking the advantage of the stepwise nature of the reaction.<sup>14,44,45</sup> Two different approaches were employed, where equivalent amounts of the PhCH<sub>2</sub>Br and PhCD<sub>2</sub>Br (molar ratio of PhCH<sub>2</sub>Br or PhCD<sub>2</sub>Br to **1** = 5:1) were added in a stepwise manner with a time interval of 20 min, but with an opposite order, in order to avoid the influences brought by the possible reactivity difference of PhCH<sub>2</sub>Br and PhCD<sub>2</sub>Br. Figure 4 shows the <sup>1</sup>H

NMR spectra of the product obtained from the H/D labeling reaction of  $1^{2-}$  with different addition order of  $\text{PhCH}_2\text{Br}$  and  $\text{PhCD}_2\text{Br}$ .

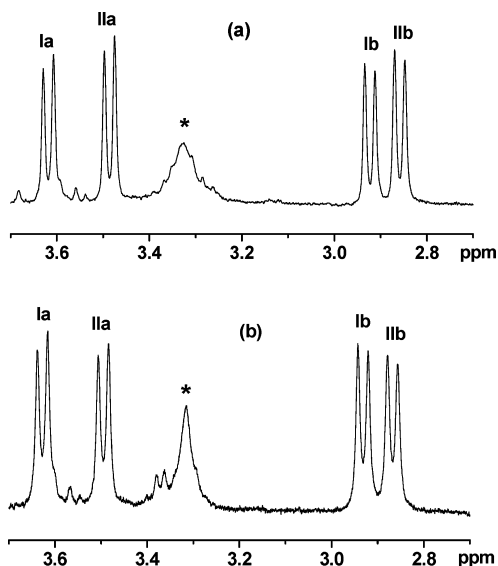


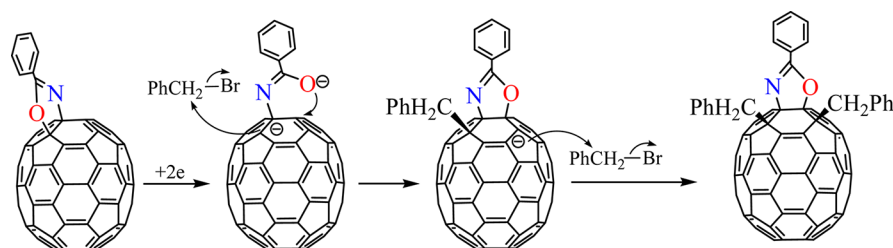
**Figure 4.**  $^1\text{H}$  NMR of the products obtained from the H/D labeling benzylation reaction of  $1^{2-}$ : (a)  $\text{PhCD}_2\text{Br}$  was added first followed by addition of equivalent amount of  $\text{PhCH}_2\text{Br}$ ; (b)  $\text{PhCH}_2\text{Br}$  was first added followed by addition of equivalent amount of  $\text{PhCD}_2\text{Br}$ . The spectrum was recorded in  $\text{CS}_2$  solution with  $\text{DMSO}-d_6$  as the external lock. The peak labeled with asterisk is due to the  $\text{H}_2\text{O}$  residue from  $\text{DMSO}$ .

As is shown in Figure 4, the intensity of the AB quartets I and II varies with the change of the addition order of  $\text{PhCD}_2\text{Br}$  and  $\text{PhCH}_2\text{Br}$ . When  $\text{PhCD}_2\text{Br}$  is added first, AB quartet I displays a less intensity (Figure 4a); while the quartet exhibits a stronger intensity when  $\text{PhCH}_2\text{Br}$  is added first (Figure 4b), indicating explicitly that the AB quartet I is related to the benzyl added during the first step, while the AB quartet II is related to the benzyl added during the second step. Considering the fact that the AB quartet I is due to the methylene protons located next to the  $\text{N}-\text{C}_{70}$  bond, while the AB quartet II is due to the methylene protons located adjacent to the  $\text{O}-\text{C}_{70}$  bond as derived from the HMBC NMR, it shows specifically that the first added benzyl group is positioned next to the  $\text{N}-\text{C}_{70}$  bond, while the second added benzyl group is placed next to the  $\text{O}-\text{C}_{70}$  bond. Notably, the intensity difference of the two AB quartets is much less significant compared to that for  $\text{C}_{60}$  counterpart,<sup>25</sup> and this is likely due to a much slower reaction rate for the first step with respect to that for the second step,<sup>46</sup> which may obscure the stepwise nature of the reaction.

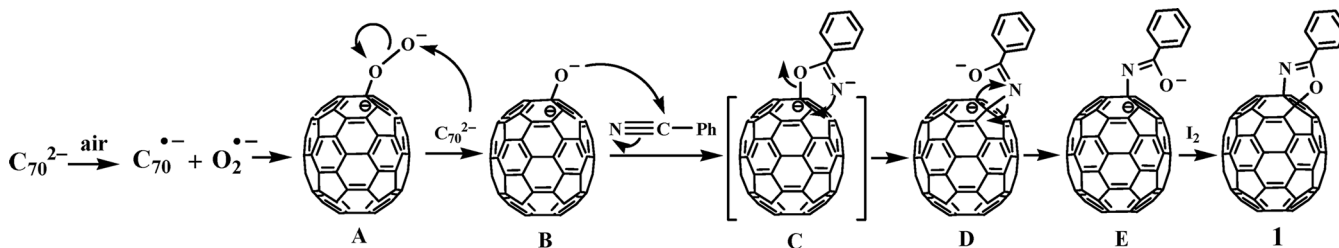
Comparing the structures of **1** to **2**, it is evident that the heteroatom on C1 of  $\text{C}_{70}$  is the one that migrates to C3 during the reaction, while the heteroatom on C2 should remain bonding to  $\text{C}_{70}$  with the formation of a singly bonded oxazolino  $\text{C}_{70}$  dianionic intermediate. For singly bonded fullerene dianionic intermediate, the available site for the next addition is usually either the *ortho*- or the *para*-position with respect to the existing addend depending on the size of the addends;<sup>45,47–52</sup> but in this case, the addition site for the first benzyl must be the C1 (the *ortho*-position relative to the remaining  $\text{X}-\text{C}_{70}$  bond at C2,  $\text{X} = \text{N}$  or  $\text{O}$ ) according to the structure of product **2**; otherwise, a *para*-addition of the benzyl group at C5 would result in a completely different compound. The result therefore indicates that the benzyl added during the first step must be positioned at C1 of  $1^{2-}$ . Since the benzylns added during the first step are shown to be added next to the  $\text{N}-\text{C}_{70}$  bond, it is rational to conclude that the N atom is the one that remains bonding to the  $\text{C}_{70}$  sphere, while the O atom is the one that migrates from C1 to C3 on the  $\text{C}_{70}$  sphere during the transformation of  $1^{2-}$  to **2**, consistent with the rearrangement result for  $\text{C}_{60}$  oxazoline dianions.<sup>25</sup> The results indicate unambiguously that compound **1** has the structure of **1a**, where the oxygen and nitrogen atoms are bonded to the C1 and C2 of  $\text{C}_{70}$ , respectively. The mechanism for the formation of **2** from  $1^{2-}$  via benzylation is proposed as shown in Scheme 2.

**Theoretical Calculations and Mechanism for the Formation of Compound 1.** Previous work on the preparation of  $\text{C}_{70}$  isoxazolines has shown that there is essentially no preference for the orientation of the isoxazolino group upon addition to the C1–C2 bond, and there is also significant amount of C5–C6 adduct formed.<sup>11</sup> The exhibited regioselectivity for the formation of **1** is therefore quite intriguing. HF (Hartree–Fock) and DFT (density functional theory) calculations were performed to probe further into the regioselective formation of **1**. Since the C1–C2, C5–C6, and C7–C21 bonds have been shown to be the preferred sites for monoaddition to  $\text{C}_{70}$ , the structures of oxazoline adducts (Figure S15, Supporting Information) at C1–C2 (**1a** and **1b**), C5–C6 (**3**), and C7–C21 bonds (**4a** and **4b**) were optimized at the HF/6-31G level with the Gaussian 03 program. The total energies for the optimized structures were calculated at the B3LYP/6-311G(d) level. The results predict that the relative energies for **1a**, **1b**, **3**, **4a**, and **4b** are 1.37, 0.00, 5.66, 19.75, and 18.99 kcal/mol, respectively. The predicted instability of **4a** and **4b** may account for the missing of any 7,21-oxazolino  $\text{C}_{70}$  regioisomer, consistent with the fact that no  $\text{C}_{70}$  isoxazolines with such configuration were obtained.<sup>11</sup> In addition, the calculations predict a significant energy increase for **3** compared to **1a** and **1b**, and a small energy difference between **1a** and **1b**,

**Scheme 2.** Proposed Mechanism for the Formation of **2** via the Reaction of  $1^{2-}$  with  $\text{PhCH}_2\text{Br}$





Scheme 3. Proposed Mechanisms for the Formation of **1** via Three-Component Reaction of  $C_{70}^{2-}$  with  $O_2$  and PhCN

implying that **1a** and **1b** are more preferred to be formed from the reaction.

Since the reaction of  $C_{60}^{2-}$  with  $O_2$  and PhCN is initiated with the activation of  $O_2$  to  $O_2^{\bullet-}$  via SET (single-electron transfer) from  $C_{60}^{2-}$ , followed by the radical combination of  $C_{60}^{\bullet-}$  and  $O_2^{\bullet-}$  to form  $C_{60}^{\bullet-}O-O^{\bullet-}$  intermediate,<sup>24</sup> while  $C_{70}$  has a very similar reductive behavior to that of  $C_{60}$ ,<sup>12</sup> it is rational that the reaction of  $C_{70}^{2-}$  with  $O_2$  and PhCN undergoes via a mechanism as illustrated in Scheme 3.

Accordingly, the reaction of  $C_{70}^{2-}$  with  $O_2$  and PhCN is initiated with the activation of  $O_2$  to  $O_2^{\bullet-}$  via SET from  $C_{70}^{2-}$ , followed by the radical combination of  $C_{70}^{\bullet-}$  and  $O_2^{\bullet-}$  to form  $C_{70}^{\bullet-}O-O^{\bullet-}$  intermediate. The  $C_{70}^{\bullet-}O-O^{\bullet-}$  peroxide is then cleaved to  $C_{70}^{\bullet-}O-O^-$  by reduction of  $C_{70}^{2-}$ , similar to the reductive cleavage of peroxides.<sup>53–55</sup> The resulting  $C_{70}^{\bullet-}O-O^-$  would then attack the nitrile bond of PhCN, with the formation of a dianionic singly bonded imine species. The anionic imine would then undergo an intramolecular nucleophilic addition back to  $C_{70}$  at the [6,6]-bond, accompanied by a heterolytic cleavage of the  $C_{70}-O$  probably due to the strong electronegativity of the oxygen atom,<sup>24,25</sup> which would result in compound **1** upon quenching with  $I_2$ , as observed for the  $C_{60}$  counterpart.<sup>24</sup>

Previous work on the reaction of  $C_{70}^{2-}$  with organic halides has shown that C2 is much more favored over C1 for the first added alkyl/aryl group,<sup>36,56</sup> resulting in predominantly 2- $RC_{70}^-$  via radical combination between  $R^{\bullet}$  and  $C_{70}^{\bullet-}$ , which are generated by the SET from  $C_{70}^{2-}$  to organic halides.<sup>14</sup> In addition, studies on the deprotonation of 1,2- $H_2C_{70}$  has shown that 2- $HC_{70}^-$  is more stable than 1- $HC_{70}^-$ , which results in the “other” regioisomer, C1-monoalkylated 1,2-dihydro[ $C_{70}$ ] derivatives, as the major product.<sup>34</sup> The results thus indicate that 2- $RC_{70}^-$  is likely much more stable than 1- $RC_{70}^-$ , which is reasonable since C2 is more strained than C1, and the addition at C2 may release more strain of the  $C_{70}$  skeleton. Consequently, the radical combination of  $C_{70}^{\bullet-}$  and  $O_2^{\bullet-}$  shown in Scheme 3 would likely result in 2- $C_{70}^{\bullet-}O-O^{\bullet-}$  (A), which would be subsequently reduced to 2- $C_{70}^{\bullet-}O-O^-$  (B) via a nucleophilic attack by  $C_{70}^{2-}$  due to the electrophilic nature of the peroxide anion.<sup>53–55</sup> The resulting 2- $C_{70}^{\bullet-}O-O^-$  (B) would then react with PhCN to form dianionic imine intermediate (C) with the O bonded to  $C_{70}$  at C2, which would result in intermediate D subsequently with the N bonded at C1. However, intermediate D (the C1-singly bonded intermediate) is likely unstable with respect to the C2-singly bonded intermediate (intermediate E) according to above discussions, and a charge-mediated rearrangement of the N from C1 to C2 for the more stable C2-intermediate is likely to occur, as reported recently for the oxazolinization of 1,4-( $PhCH_2$ )<sub>2</sub> $C_{60}$ .<sup>30</sup> Such an anion-initiated rearrangement of nitrogen atom has also been shown as the evidence for the participation of an anion pathway during Neber rearrangement.<sup>57</sup>

Computational calculations on the stability of C1-, C2-, and C5-singly bonded intermediates provide further rationality for the regioselective formation of compound **1**. The structures of C1-, C2-, and C5-singly bonded intermediates were optimized at the HF/6-31G level, while the energy calculations were performed at the B3LYP/6-311G(d) level. The calculations predict the relative energies are 2.26, 0.00, and 1.90 kcal/mol for the C1-, C2-, and C5- $C_{70}^-O_2^-$  intermediates; 8.83, 0.00, and 3.70 kcal/mol for the C1-, C2-, and C5- $C_{70}^-O^-$  intermediates; and 8.13, 0.00, and 4.17 kcal/mol for C1-, C2-, and C5- $C_{70}^-NC(Ph)O^-$ . The results suggest a significant stability for the C2-singly bonded  $C_{70}$  intermediates with respect to the C1- and C5-singly bonded ones, which are consistent with the experimental results as observed previously,<sup>34,36,56</sup> and may account for the preferred formation of **1a** over **1b** and **3** from the reaction, even though **1b** is predicted to be more stable than **1a** by 1.37 kcal/mol.

**UV-vis of Compound 2.** Since the UV-vis absorptions for fullerene adducts are sensitive toward the addition pattern rather than the type of the addends, it is of interest to examine the UV-vis absorptions of the *cis*-1  $C_{70}$  adduct with respect to the apical pentagon. Figure 5 shows the UV-vis spectrum of **2**

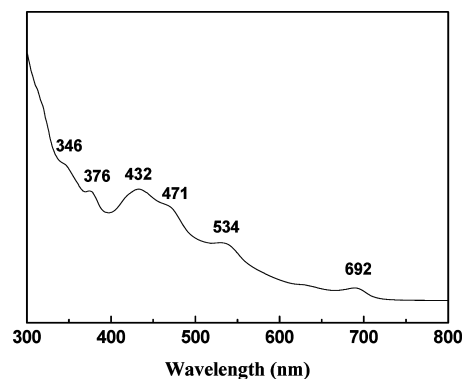
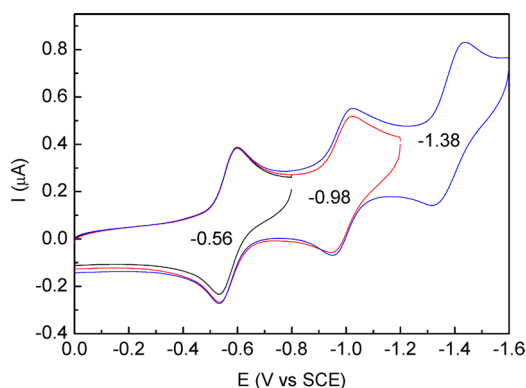


Figure 5. UV-vis spectrum of compound **2** recorded in toluene.

recorded in toluene. Absorptions at 346, 376, 432, 471, 534, and 692 nm are shown. Notably, the absorption onset for the  $C_{70}$  *cis*-1 adduct is extended to around 739 nm from 650 nm for  $C_{70}$ ,<sup>58</sup> even though the  $\pi$ -conjugation of **2** is decreased with respect to that of  $C_{70}$  ( $66\pi$  vs  $70\pi$ ) by the addition of addends. A similar red-shift of the UV-vis absorptions is observed for  $C_{60}$  derivatives compared with that of  $C_{60}$ ,<sup>59,60</sup> where the  $\pi$ -conjugation is also ruptured upon derivatization, demonstrating a unique aspect of the electronic structures for the 3-D conjugated systems.

**Cyclic Voltammetry of Compound 2.** Figure 6 shows the cyclic voltammogram of **2** recorded in PhCN containing 0.1 M TBAP with a scan rate of 0.1 V/s. The compound exhibits three



**Figure 6.** Cyclic voltammograms of compound **2** in PhCN containing 0.1 M TBAP with a scan rate of 0.1 V/s.

quasi-reversible redox processes with  $E_{1/2}$  at  $-0.56$ ,  $-0.98$ , and  $-1.38$  V vs SCE, which are negatively shifted by about 80–140 mV with respect to those of  $C_{70}$  ( $-0.45$ ,  $-0.85$ , and  $-1.30$  V vs SCE) measured under the same conditions, probably due to the cleavage of the conjugated  $\pi$ -electrons in the polar region of  $C_{70}$ . As for compound **1** (Figure S6, Supporting Information), the first redox process is quasi-reversible, with  $E_{1/2}$  at  $-0.46$  V vs SCE, almost identical to that of  $C_{70}$ , in agreement with the reduction potentials for  $C_{70}$  isoxazolines reported previously.<sup>11</sup> However, further reduction of **1** is complicated due to the reductive cleavage of the  $C_{70}$ –O bond. The results indicate that the addition of benzyl groups next to the oxazoline cycle on  $C_{70}$  sphere can stabilize the heterocycle upon reduction, as observed for the  $C_{60}$  counterpart.<sup>43</sup>

## CONCLUSIONS

We have shown a regioselective oxazolation of  $C_{70}^{2-}$  via a three-component reaction of  $C_{70}^{2-}$ ,  $O_2$ , and PhCN, and the formation of a  $C_{70}$  derivative with *cis*-1 configuration with respect to the apical pentagon with subsequent benzylation. The UV-vis and electrochemical properties of the *cis*-1  $C_{70}$  adduct are examined. A reaction mechanism accounting for the regiochemistry of **1** is proposed on the basis of previous reports and computational calculations. The results indicate that the regiochemistry of the oxazolation of  $C_{70}^{2-}$  is controlled by the stability of both the products and the singly-bonded anionic intermediates, which may be helpful in gaining a better understanding on the regioselectivity for functionalization of fullerenes with a lower symmetry.

## EXPERIMENTAL SECTION

**General Methods.** TBAP was recrystallized from absolute ethanol and dried under vacuum at 313 K prior to use. All reactions were performed under argon atmosphere unless otherwise noted. Benzonitrile (PhCN) was distilled over  $P_2O_5$  under vacuum at 305 K prior to use. All of the other reagents and solvents were obtained commercially and used as received.

Controlled-potential bulk electrolysis was carried out on a potentiostat/galvanostat using an “H” type cell which consisted of two platinum gauze electrodes (working and counter electrodes) separated by a sintered glass frit. A three-electrode cell was used for CV measurements and a glassy carbon, a platinum and a saturated calomel electrode (SCE) were used as working electrode, counter electrode and reference electrode. A fritted-glass bridge of low porosity which contained the solvent/supporting electrolyte mixture was used to separate the SCE from the bulk of the solution.

**Synthesis of Compound 1.** Typically,  $C_{70}$  (80 mg, 95.2  $\mu$ mol) was electrolyzed at  $-1.00$  V vs SCE in 50 mL freshly distilled PhCN

solution containing 0.1 M TBAP under argon at 30 °C. The potentiostat was switched off when the conversion of  $C_{70}$  to  $C_{70}^{2-}$  was completed. A total of 60 mL of air was injected into the solution along with the flow of argon. The air was introduced via a stepwise manner, where 20 mL of air was introduced during each step by about 15 s, the flow of argon was then stopped for about 1 min. The procedures were repeated for three times, with the system being put under argon after the completion of air introduction. The solution was then oxidized back to neutral by reacting with  $I_2$  (1.22 g, 4.81 mmol) for 1.5 h.

The solvent was removed under reduced pressure, and the residue was washed with methanol to remove TBAP and unreacted  $I_2$ . The obtained crude product was purified using a Buckyprep HPLC column eluted with toluene at a flow rate of 3.7 mL/min and the detector wavelength was set at 380 nm. Compound **1** was obtained with an isolated yield of 16% (15 mg) along with 17 mg of unreacted  $C_{70}$ . The rest of the reaction mixture was insoluble in toluene or  $CS_2$ , and was likely due to the polymerization reaction involving  $C_{70}$  epoxide species, similar to the case for  $C_{60}$  epoxides.<sup>26,27</sup>

**Spectral Characterization of Compound 1.** Positive ESI FT-ICR MS,  $m/z$  calcd for  $C_{77}H_6NO$  [ $M + H$ ]<sup>+</sup>: 960.04439, found 960.04616. <sup>1</sup>H NMR (600 MHz, in  $CS_2$ , DMSO- $d_6$  was used as the external lock solvent):  $\delta$  7.94 (d, 2H), 7.35 (t, 1H), 7.27 (t, 2H). <sup>13</sup>C NMR (150 MHz, in  $CS_2$ , DMSO- $d_6$  was used as the external lock solvent):  $\delta$  162.48 (1C, C=N), 154.05 (2C), 150.74 (2C), 150.56 (1C), 150.42 (2C), 150.24 (2C), 149.84 (2C), 149.69 (2C), 149.45 (2C), 149.23 (2C), 148.91 (2C), 148.60 (2C), 148.44 (2C), 148.21 (2C), 147.76 (2C), 146.98 (2C), 146.78 (2C), 146.69 (2C), 146.46 (1C), 146.38 (2C), 145.80 (2C), 145.19 (2C), 145.09 (2C), 143.61 (2C), 143.34 (2C), 142.93 (2C), 142.80 (2C), 142.74 (2C), 139.39 (2C), 139.34 (2C), 138.46 (2C), 132.78 (2C), 132.05 (2C), 131.80 (2C), 131.68 (Ph, 1C), 130.77 (2C), 130.67 (2C), 128.56 (Ph, 2C), 128.03 (Ph, 2C), 125.91 (Ph, 1C), 92.97 (1C,  $sp^3$ , C–O), 86.67 (1C,  $sp^3$ , C–N); UV-vis (toluene)  $\lambda_{max}/nm$ : 340, 400, 465, 538, 660.

**Synthesis of Compound 2. Method A.** Typically,  $C_{70}$  (50 mg, 59.5  $\mu$ mol) was electrolyzed at  $-1.00$  V vs SCE in 50 mL of freshly distilled PhCN solution containing 0.1 M TBAP under argon at 30 °C. The potentiostat was switched off when the conversion of  $C_{70}$  to  $C_{70}^{2-}$  was completed. Then 60 mL of air was injected into the solution along with the flow of argon, following similar procedures for preparing **1**. Then 40-fold PhCH<sub>2</sub>Br (283  $\mu$ L) was added to the solution. The reaction was allowed to proceed for 4 h with stirring under argon. The workup for the purification of compound **2** is similar to that for compound **1**. Compound **2** was obtained with an isolated yield of 22% (15 mg) along with 2.3 mg of unreacted  $C_{70}$ . The rest of the reaction mixture was insoluble in toluene or  $CS_2$ , and was likely due to the polymerization reaction involving  $C_{70}$  epoxide species. **Method B.** Compound **1** (16 mg, 16.7  $\mu$ mol) was electrolyzed at  $-1.00$  V vs SCE in 15 mL of freshly distilled benzonitrile solution containing 0.1 M TBAP under argon. Then 40-fold of benzyl bromide (79  $\mu$ L) was added to the anionic solution when the conversion of **1** to  $I^{2-}$  was completed. The reaction was allowed to proceed for 3 h. The workup for isolation is the same as that for compound **1**. The HPLC trace of the crude product (Figure S7b, Supporting Information) shows the formation of compound **2**, along with  $C_{70}$ , which is likely produced due to the decomposition of the  $I^{2-}$  and 1,2-H(PhCH<sub>2</sub>) $C_{70}$  (judging by HPLC retention time), which is likely generated by the reaction of  $C_{70}^{2-}$  with PhCH<sub>2</sub>Br and H<sub>2</sub>O residue in the solvent.<sup>36</sup> Compound **2** was obtained with an isolated yield of 37% (7.1 mg) along with about 2.1 mg of  $C_{70}$  and 2 mg of 1,2-H(PhCH<sub>2</sub>) $C_{70}$ .

**H/D Labeling Benzylation of  $I^{2-}$ .** Equivalent amounts of PhCD<sub>2</sub>Br (molar ratio, PhCD<sub>2</sub>Br:**1** = 5:1) and PhCH<sub>2</sub>Br (molar ratio, PhCH<sub>2</sub>Br:**1** = 5:1) were added to the  $I^{2-}$  solution via a stepwise manner with a time interval of 20 min. Opposite addition orders were employed to eliminate the difference caused by the possible reactivity difference between PhCD<sub>2</sub>Br and PhCH<sub>2</sub>Br.

**Spectral Characterization of Compound 2.** Positive ESI FT-ICR MS,  $m/z$  calcd for  $C_{91}H_{19}NO$  [ $M + H$ ]<sup>+</sup>: 1142.15394, found 1142.15532. <sup>1</sup>H NMR (600 MHz;  $CS_2$  with DMSO- $d_6$  as the external lock):  $\delta$  7.99 (d, 2H), 7.39 (t, 1H), 7.34 (t, 2H), 6.79 to 6.72 (m, 10H), 3.30 (ABq,  $\Delta\nu_{AB}$  = 421 Hz,  $J_{AB}$  = 13.2 Hz), 3.21 (ABq,  $\Delta\nu_{AB}$  =

382 Hz,  $J_{AB} = 13.2$  Hz);  $^{13}\text{C}$  NMR (150 MHz,  $\text{CS}_2$  with  $\text{DMSO}-d_6$  as the external lock):  $\delta$  164.65 (1C), 163.13 (1C), 161.47 (1C, C=N), 153.67 (1C), 150.58 (1C), 150.46 (2C), 150.36 (1C), 150.02 (1C), 149.86 (1C), 149.74 (1C), 149.33 (1C), 149.26 (3C), 149.14 (2C), 149.03 (1C), 148.99 (1C), 148.86 (1C), 148.84 (1C), 148.81 (1C), 148.71 (1C), 148.60 (1C), 148.58 (1C), 148.54 (1C), 148.46 (1C), 148.24 (1C), 147.83 (1C), 147.77 (2C), 147.69 (1C), 147.38 (1C), 147.32 (1C), 146.91 (1C), 146.75 (1C), 146.63 (1C), 146.43 (2C), 146.37 (1C), 146.04 (1C), 145.93 (1C), 145.41 (1C), 144.04 (2C), 143.10 (1C), 142.83 (1C), 142.69 (1C), 142.21 (1C), 140.95 (1C), 140.76 (1C), 140.67 (1C), 140.43 (1C), 139.51 (1C), 139.47 (1C), 139.36 (1C), 138.51 (1C), 136.78 (1C), 136.00 (1C), 133.93 (1C), 133.66 (1C), 132.97 (1C), 132.80 (1C), 131.68 (1C), 131.47 (Ph, 1C), 131.39 (1C), 131.37 (1C), 131.04 (1C), 130.99 (Ph, 2C), 130.75 (Ph, 2C), 130.39 (Ph, 1C), 129.90 (Ph, 1C), 128.20 (Ph, 2C), 128.11 (Ph, 2C), 127.27 (Ph, 2C), 127.10 (Ph, 2C), 127.03 (Ph, 1C), 126.43 (Ph, 1C), 126.19 (Ph, 1C), 92.46 (1C,  $\text{sp}^3$ , C-O), 84.95 (1C,  $\text{sp}^3$ , C-N), 57.68 (1C, C- $\text{CH}_2\text{Ph}$ ), 57.00 (1C, C- $\text{CH}_2\text{Ph}$ ), 42.99 (1C,  $\text{CH}_2$ ), 41.92 (1C,  $\text{CH}_2$ ); UV-vis (toluene)  $\lambda_{\text{max}}/\text{nm}$ : 346, 376, 432, 471, 534, 692.

**X-ray Single-Crystal Diffraction of Compound 2.** Black leaf-shaped crystals of compound 2 suitable for X-ray analysis were obtained by slowly diffusing hexane into  $\text{CS}_2$  solution of compound 2 at room temperature. Single-crystal X-ray diffraction data were collected using graphite-monochromated Mo  $K\alpha$  radiation ( $\lambda = 0.71073$  Å) in the range  $1.47^\circ < \theta < 26.05^\circ$ . The structure was solved with the direct methods using SHELXS-97 and refined with full-matrix least-squares techniques using the SHELXL-97 program within WINGX. Nonhydrogen atoms were refined anisotropically. Crystal data of 2:  $\text{C}_{21}\text{H}_{19}\text{NO}$ ,  $M_w = 1142.07$ , dark, orthorhombic, space group  $P2(1)2(1)2(1)$ ,  $a = 11.203$  Å,  $b = 15.093$  Å,  $c = 27.684$  Å,  $\alpha = 90.00^\circ$ ,  $\beta = 90.00^\circ$ ,  $\gamma = 90.00^\circ$ ,  $V = 4681.0$  Å $^3$ ,  $z = 4$ ,  $D_{\text{calcd}} = 1.621$  Mg m $^{-3}$ ,  $\mu = 0.095$  mm $^{-1}$ ,  $T = 293(2)$  K, crystal size  $0.34 \times 0.30 \times 0.07$  mm $^3$ ; reflections collected 26376, independent reflections 9219; 6849 with  $I > 2\sigma(I)$ ;  $R_1 = 0.0578$  [ $I > 2\sigma(I)$ ],  $wR_2 = 0.1136$  [ $I > 2\sigma(I)$ ];  $R_1 = 0.0865$  (all data),  $wR_2 = 0.1279$  (all data), GOF (on  $F^2$ ) = 0.954.

## ■ ASSOCIATED CONTENT

### ■ Supporting Information

X-ray crystallographic files for compound 2 (CIF), HPLC of the crude product, HRMS,  $^1\text{H}$  and  $^{13}\text{C}$  NMR spectra of compounds 1 and 2, HMBC NMR spectrum of compound 2,  $^1\text{H}$  NMR of deuterated compound 2, and calculation details. This material is available free of charge via the Internet at <http://pubs.acs.org/>.

## ■ AUTHOR INFORMATION

### ■ Corresponding Author

\*E-mail: [xgao@ciac.jl.cn](mailto:xgao@ciac.jl.cn).

### ■ Notes

The authors declare no competing financial interest.

## ■ ACKNOWLEDGMENTS

The work was supported by the National Natural Science Foundation of China (20972150, 21172212) and the Solar Energy Initiative of the Chinese Academy of Sciences (KGCX2-YW-399 + 9).

## ■ REFERENCES

- Hirsch, A.; Brettreich, M. *Fullerenes: Chemistry and Reactions*; Wiley-VCH: Weinheim, 2005.
- Bingel, C. *Chem. Ber.* **1993**, *126*, 1957–1959.
- Herrmann, A.; Rüttimann, M.; Thilgen, C.; Diederich, F. *Helv. Chim. Acta* **1995**, *78*, 1673–1704.
- Prato, M.; Maggini, M. *Acc. Chem. Res.* **1998**, *31*, 519–526.
- Wilson, S. R.; Lu, Q. *J. Org. Chem.* **1995**, *60*, 6496–6498.
- Belik, P.; Gügel, A.; Spickermann, J.; Müllen, K. *Angew. Chem., Int. Ed. Engl.* **1993**, *32*, 78–80.
- Herrmann, A.; Diederich, F.; Thilgen, C.; Meer, H.-U.; Müller, W. H. *Helv. Chim. Acta* **1994**, *77*, 1689–1706.
- Henderson, C. C.; Cahill, P. A. *Science* **1993**, *259*, 1885–1887.
- Spielmann, H. P.; Wang, G.-W.; Meier, M. S.; Weedon, B. R. *J. Org. Chem.* **1998**, *63*, 9865–9871.
- Meier, M. S.; Poplawska, M. *J. Org. Chem.* **1993**, *58*, 4524–4525.
- Meier, M. S.; Poplawska; Compton, A. L.; Shaw, J. P.; Selegue, J. P.; Guarr, T. F. *J. Am. Chem. Soc.* **1994**, *116*, 7044–7048.
- Xie, Q.; Ptrez-Cordero, E.; Echegoyen, L. *J. Am. Chem. Soc.* **1992**, *114*, 3978–3980.
- Caron, C.; Subramanian, R.; D'Souza, F.; Kim, J.; Kunter, W.; Jones, M. T.; Kadish, K. M. *J. Am. Chem. Soc.* **1993**, *115*, 8505–8506.
- Kadish, K. M.; Gao, X.; Gorelik, O.; Van Caemelbecke, E.; Suenobu, T.; Fukuzumi, S. *J. Phys. Chem. A* **2000**, *104*, 2902–2907.
- Meier, M. S.; Bergosh, R. G.; Gallagher, M. E.; Spielmann, H. P.; Wang, Z. *J. Org. Chem.* **2002**, *67*, 5946–5952.
- Thilgen, C.; Diederich, F. *Top. Curr. Chem.* **1999**, *199*, 135–171.
- Xiao, Z.; Wang, F.; Huang, S.; Gan, L.; Zhou, J.; Yuan, G.; Lu, M.; Pan, J. *J. Org. Chem.* **2005**, *70*, 2060–2066.
- Maroto, E. E.; de Cózar, A.; Filippone, S.; Martín-Domenech, Á.; Suarez, M.; Cossio, F. P.; Martín, N. *Angew. Chem., Int. Ed.* **2011**, *50*, 6060–6064.
- Hirsch, A. *Top. Curr. Chem.* **1999**, *199*, 1–65.
- Meng, X.; Zhang, W.; Tan, Z.; Du, C.; Li, C.; Bo, Z.; Li, Y.; Yang, X.; Zhen, M.; Jiang, F.; Zheng, J.; Wang, T.; Jiang, L.; Shu, C.; Wang, C. *Chem. Commun.* **2012**, *48*, 425–427.
- Meng, X.; Zhang, W.; Tan, Z.; Li, Y.; Ma, Y.; Wang, T.; Jiang, L.; Shu, C.; Wang, C. *Adv. Funct. Mater.* **2012**, *22*, 2187–2193.
- Zheng, M.; Li, F.-F.; Ni, L.; Yang, W.-W.; Gao, X. *J. Org. Chem.* **2008**, *73*, 3159–3168.
- Li, F.-F.; Yang, W.-W.; He, G.-B.; Gao, X. *J. Org. Chem.* **2009**, *74*, 8071–8077.
- Hou, H.-L.; Gao, X. *J. Org. Chem.* **2012**, *77*, 2553–2558.
- Yang, W.-W.; Li, Z.-J.; Li, F.-F.; Gao, X. *J. Org. Chem.* **2011**, *76*, 1384–1389.
- Winkler, K.; Costa, D. A.; Balch, A. L.; Fawcett, W. R. *J. Phys. Chem.* **1995**, *99*, 17431–17436.
- Krinichnaya, E. P.; Moravsky, A. P.; Efimov, O.; Sobczak, J. W.; Winkler, K.; Kutner, W.; Balch, A. L. *J. Mater. Chem.* **2005**, *15*, 1468–1476.
- Liu, T.-X.; Wang, G.-W. *J. Org. Chem.* **2008**, *73*, 6417–6420.
- Chang, W.-W.; Li, Z.-J.; Yang, W.-W.; Gao, X. *Org. Lett.* **2012**, *14*, 2386–2389.
- Li, Z.-J.; Li, F.-F.; Li, S.-H.; Chang, W.-W.; Yang, W.-W.; Gao, X. *Org. Lett.* **2012**, *14*, 3482–3485.
- For the numbering of  $\text{C}_{70}$ , refer to: Godly, E. W.; Taylor, R. *Pure Appl. Chem.* **1997**, *69*, 1411–1434.
- Smith, A. B., III; Strongin, R. M.; Brard, L.; Furst, G. T.; Romanow, W. J.; Owens, K. G.; Goldschmidt, R. J.; King, R. C. *J. Am. Chem. Soc.* **1995**, *117*, 5492–5502.
- Meier, M. S.; Kiegiel, J. *Org. Lett.* **2001**, *3*, 1717–1719.
- Wang, Z.; Meier, M. S. *J. Org. Chem.* **2004**, *69*, 2178–2180.
- Wang, G.-W.; Yang, H.-T.; Wu, P.; Wang, C.-Z. *Eur. J. Org. Chem.* **2010**, 5714–5721.
- Ni, L.; Chang, W.; Hou, H.-L.; Li, Z.-J.; Gao, X. *Org. Biomol. Chem.* **2011**, *9*, 6646–6653.
- Zhang, X.; Foote, C. S. *J. Am. Chem. Soc.* **1995**, *117*, 4271–4275.
- Meier, M. S.; Spielmann, H. P.; Bergosh, R. G.; Haddon, R. C. *J. Am. Chem. Soc.* **2002**, *124*, 8090–8094.
- Wang, G.-W.; Li, F.-B.; Chen, Z.-X.; Wu, P.; Cheng, B.; Xu, Y. *J. Org. Chem.* **2007**, *72*, 4779–4783.
- Wang, G.-W.; Li, F.-B.; Xu, Y. *J. Org. Chem.* **2007**, *72*, 4774–4778.
- Shen, C. K.-F.; Yu, H.-h.; Juo, C.-G.; Chien, K.-M.; Her, G.-R.; Luh, T.-Y. *Chem.—Eur. J.* **1997**, *3*, 744–748.



- (42) Delgado, J. L.; Cardinali, F.; Espíldora, E.; Torres, M. R.; Langa, F.; Martín, N. *Org. Lett.* **2008**, *10*, 3705–3708.
- (43) Li, F.-F.; Gao, X.; Zheng, M. *J. Org. Chem.* **2009**, *74*, 82–87.
- (44) Subramanian, R.; Kadish, K. M.; Vijayashree, M. N.; Gao, X.; Jones, M. T.; Miller, D. M.; Krause, K.; Suenobu, T.; Fukuzumi, S. *J. Phys. Chem.* **1996**, *100*, 16327–16335.
- (45) Fukuzumi, S.; Suenobu, T.; Hirasaka, T.; Arakawa, R.; Kadish, K. M. *J. Am. Chem. Soc.* **1998**, *120*, 9220–9227.
- (46) When benzyl bromide was added to C<sub>60</sub> oxazoline dianion solution, the solution color changed quickly from red to green and then gradually to brown, demonstrating a well-defined stepwise nature of the reaction; however, when benzyl bromide was added to C<sub>70</sub> oxazoline dianion solution, no color change was observed throughout the reaction, suggesting that the stepwise nature of the reaction is rather indistinctive for the reaction.
- (47) Komatsu, K.; Murata, Y.; Takimoto, N.; Mori, S.; Sugita, N.; Wan, T. S. M. *J. Org. Chem.* **1994**, *59*, 6101–6102.
- (48) Komatsu, K.; Takimoto, N.; Murata, Y.; Wan, T. S. M.; Wong, T. *Tetrahedron Lett.* **1996**, *37*, 6153–6156.
- (49) Allard, E.; Cheng, F.; Chopin, S.; Delaunay, J.; Rondeaub, D.; Cousseau, J. *New J. Chem.* **2003**, *27*, 188–192.
- (50) Yang, W.-W.; Li, Z.-J.; Gao, X. *J. Org. Chem.* **2010**, *75*, 4086–4094.
- (51) Cheng, F.; Murata, Y.; Komatsu, K. *Org. Lett.* **2002**, *4*, 2541–2544.
- (52) Yang, W.-W.; Li, Z.-J.; Gao, X. *J. Org. Chem.* **2011**, *76*, 6067–6074.
- (53) Gilchrist, T. L. In *Comprehensive Organic Synthesis: Selectivity, Strategy & Efficiency in Modern Organic Chemistry, Vol. 8, Reduction*; Trost, B. M., Fleming, I., Eds.; Pergamon Press: Oxford, 1991; p 396.
- (54) Boche, G.; Lohrenz, J. C. W. *Chem. Rev.* **2001**, *101*, 697–756.
- (55) Nobe, Y.; Arayama, K.; Urabe, H. *J. Am. Chem. Soc.* **2005**, *127*, 18006–18007.
- (56) Wang, Z.; Meier, M. S. *J. Org. Chem.* **2003**, *68*, 3043–3048.
- (57) Ooi, T.; Takahashi, M.; Doda, K.; Maruoka, K. *J. Am. Chem. Soc.* **2002**, *124*, 7640–7641.
- (58) Ajie, H.; Alvarez, M. M.; Anz, S. J.; Beck, R. D.; Diederich, F.; Fostiropoulos, K.; Huffman, D. R.; Krätschmer, W.; Rubin, Y.; Schriver, K. E.; Sensharma, D.; Whetten, R. L. *J. Phys. Chem.* **1990**, *94*, 8630–8633.
- (59) Guldi, D. M.; Asmus, K.-D. *J. Phys. Chem. A* **1997**, *101*, 1472–1481.
- (60) Li, Z.-J.; Yang, W.-W.; Gao, X. *J. Phys. Chem. A* **2011**, *115*, 6432–6437.